



## Article

# Study of Atmospheric Aerosol in the Baikal Mountain Basin with Shipborne and Ground-Based Lidars

Sergei Nasonov \*, Yurii Balin, Marina Klemasheva, Grigorii Kokhanenko, Mikhail Novoselov and Ioganes Penner

V.E. Zuev Institute of Atmospheric Optics, Siberian Branch, Russian Academy of Sciences, 634055 Tomsk, Russia; balin@iao.ru (Y.B.); marina@iao.ru (M.K.); kokh@iao.ru (G.K.); novoselov@iao.ru (M.N.); penner@iao.ru (I.P.)

\* Correspondence: nsvtsk@iao.ru; Tel.: +7-3-822-491-283

**Abstract:** The results of long-term lidar studies of the peculiarities of the vertical structure of atmospheric aerosols over Lake Baikal are presented. The paper provides an analysis of data obtained over the period from 2010 to 2022. The studies were carried out under both the background conditions and the extreme natural conditions associated with severe wildfires in Siberia. The parameters of the lidars used in regular summer expeditions to Lake Baikal are briefly described. The data analysis shows that the vertical structure of the aerosol in the lower troposphere up to 2000 m above Baikal in summer is often a stable structure of several aerosol layers tens to hundreds of meters thick. There can be no mixing of layers because the water in the lake is very cold and the aerosol does not rise to higher layers while the air is warming up during the day. The difference is shown between the spatiotemporal structures of aerosol plumes from local wildfires within the lake area and from distant sources. The Angstrom parameter and the aerosol optical depth are calculated for different atmospheric conditions:  $\eta_{\beta} = 1.57 \pm 0.16$  and  $\tau = 0.09$  for background conditions;  $\eta_{\beta} = 1.41 \pm 0.07$  and  $\tau = 0.64$  for the cases of the observation of smoke aerosol from distant wildfires; and  $\eta_{\beta} = 1.05 \pm 0.08$  and  $\tau = 0.25$  for the cases of the observation of smoke aerosol from nearby wildfires.

**Keywords:** aerosol; lidar; Lake Baikal; meteorological parameters; Boyarsky stationary site; shipping; wildfires



**Citation:** Nasonov, S.; Balin, Y.; Klemasheva, M.; Kokhanenko, G.; Novoselov, M.; Penner, I. Study of Atmospheric Aerosol in the Baikal Mountain Basin with Shipborne and Ground-Based Lidars. *Remote Sens.* **2023**, *15*, 3816. <https://doi.org/10.3390/rs15153816>

Academic Editor: Manuel Antón

Received: 27 June 2023

Revised: 28 July 2023

Accepted: 28 July 2023

Published: 31 July 2023



**Copyright:** © 2023 by the authors. Licensee MDPI, Basel, Switzerland. This article is an open access article distributed under the terms and conditions of the Creative Commons Attribution (CC BY) license (<https://creativecommons.org/licenses/by/4.0/>).

## 1. Introduction

For many years, scientific research has been carried out on Lake Baikal in terms of global environmental and climate changes [1–10]. The specificity of the Baikal region is the permanent water–land temperature contrast during the open water period, which affects the lower part of the atmospheric boundary layer (ABL) and determines the generation of heat fluxes, primarily during the day. In addition, though the region is located in the western transport zone, the characteristic regional meteorological conditions, mainly the wind system and the associated cloudiness and precipitation regimes, are due to the mountains surrounding the lake [11].

Baikal Lake is surrounded on all sides by high mountain ranges. The Primorsky and Baikal mountains spread along the western coast of the lake. The highest point of the Primorsky Ridge is 1746 m. The highest point of the Baikal Ridge is 2588 m. The southern part of the eastern shore of Baikal Lake is covered by the Khamar-Daban Mountain. Its maximum height is 2371 m. The highest of the Baikal ranges—Barguzinsky—lies to the northeast of Khamar-Daban. The height of the maximum point of the Barguzinsky range is 2841 m. The average height of the mountains surrounding Baikal Lake is 887 m.

The territory of the Baikal region is remote from oceans and seas and is located at the latitude of a sharply continental climate, with long, cold winters and a relatively warm summer period [12]. In winter, the circulation of air masses in the atmosphere is characterized by high atmospheric pressure (Asian anticyclone) with clear, sunny, and

frosty weather and the development of cooling processes (temperature inversions). In the summer season, there is an increase in cyclonic activity with the arrival of continental and Atlantic air masses from the west, bringing the main amount of precipitation. Central Asian continental dry and warm air masses come from the south and southwest. In the second half of summer, there is an activation of southern cyclones, bringing humid air masses through northern Mongolia. The water area of the lake has a length exceeding 600 km; so, in different areas the conditions can vary greatly in terms of the distribution of precipitation and air temperature. The specific features of the climate of this region are caused primarily by orographic factors. Due to the elongation of the lake from northeast to southwest and the complex mountainous terrain surrounding the lake on all sides, with many gorges and intermountain basins, local winds like Sarma, Barguzin, Verkhovik, and Kultuk act here. They affect the spatial distribution and transport of atmospheric aerosol over the water area of the lake. A large volume of the lake's water, which slowly heats up and cools down, influences the climate of the coastal area. This fact significantly softens the continentality of the climate compared to that of the neighboring territories and determines the relatively cold summers and warm winters.

The Baikal water area is large; therefore, a significant amount of aerosol impurities can enter the lake from the atmosphere. Therefore, the atmospheric aerosol plays a key part in the formation of the chemical composition of the Baikal water and determines the Baikal water quality. Due to the gyral circulation in the Baikal mountain basin [13], impurities which enter the atmosphere can be transported throughout the water area, contributing to the pollution of the hydrosphere of the region. Moreover, pollutants not only from local sources but also from the vast territories of Siberia, China, and Mongolia can be accumulated in the mountain basin. All these processes need to be studied in order to predict the environmental changes in the region in terms of the negative impact on the unique natural objects [14].

Every year the anthropogenic impact on the Baikal environment is actively increasing. One of the main sources of the impurities entering the atmosphere above the lake is the emissions from the large thermal power plants located in the nearest cities of the Baikal region and the small boiler houses in the water protection zone that use coal [3]. Industrial enterprises also contribute to the pollution of this region [15]. A serious threat to the ecological safety of Lake Baikal is the ever-increasing anthropogenic load on the environment due to the large flow of tourists. During the coronavirus pandemic, due to the restrictive measures introduced, the number of tourists significantly decreased and, as shown in [16], in 2022 the background values of aerosol and gaseous impurities were recorded in the atmosphere. During this period, the main contribution to atmospheric pollution was made by nearby local sources located near the coastal zone of the lake.

One of significant sources of pollution of the Baikal atmosphere and hydrosphere is smoke aerosol emitted during Siberian wildfires, primarily in the Irkutsk region, the Republic of Buryatia, the Krasnoyarsk Territory, and Yakutia, which causes strong damage to the regional ecosystem. In the past years, the smoke aerosol over the Baikal water area has been studied on almost every expedition, primarily because of the climate warming in the region [17].

Lidars are among the most promising tools for atmospheric research. They allow quick and remote acquisition of required information with high spatial and temporal resolution.

In this paper, we present the results of long-term experimental lidar studies of features of the spatiotemporal structure of the atmospheric aerosol over Lake Baikal, under both the background and the extreme conditions associated with severe wildfires in Siberia. The results of this work are of great importance for predicting and preventing possible climate and environmental changes occurring in the world's largest freshwater body with a many endemic plant and animal species.

## 2. Equipment and Techniques

Figure 1 shows a map of Lake Baikal. Lake Baikal is located in the eastern part of Russia, on the border of the Irkutsk region (on the western side) and the Republic of Buryatia (on the eastern side). The length of the lake from south to north is 636 km, and the width is up to 80 km. The map shows the elevation changes of the surrounding mountains and the locations of the main administrative centers of the regions adjacent to Lake Baikal (Irkutsk and Ulan-Ude). Instrumental research on the state of the atmosphere in the Baikal region was carried out both at the stationary points shown on the map (Listvyanka, Bolshiye Koty, and Boyarsky) [2,4,5] and from mobile carriers: aircraft, research ships, and cars [6,18,19]. Ground-based and shipborne lidar studies of the atmosphere over Lake Baikal were regularly carried out with the participation of the authors of this work using LOSA lidars (Figure 1) designed at the Institute of Atmospheric Optics, Siberian Branch, Russian Academy of Sciences [20,21].

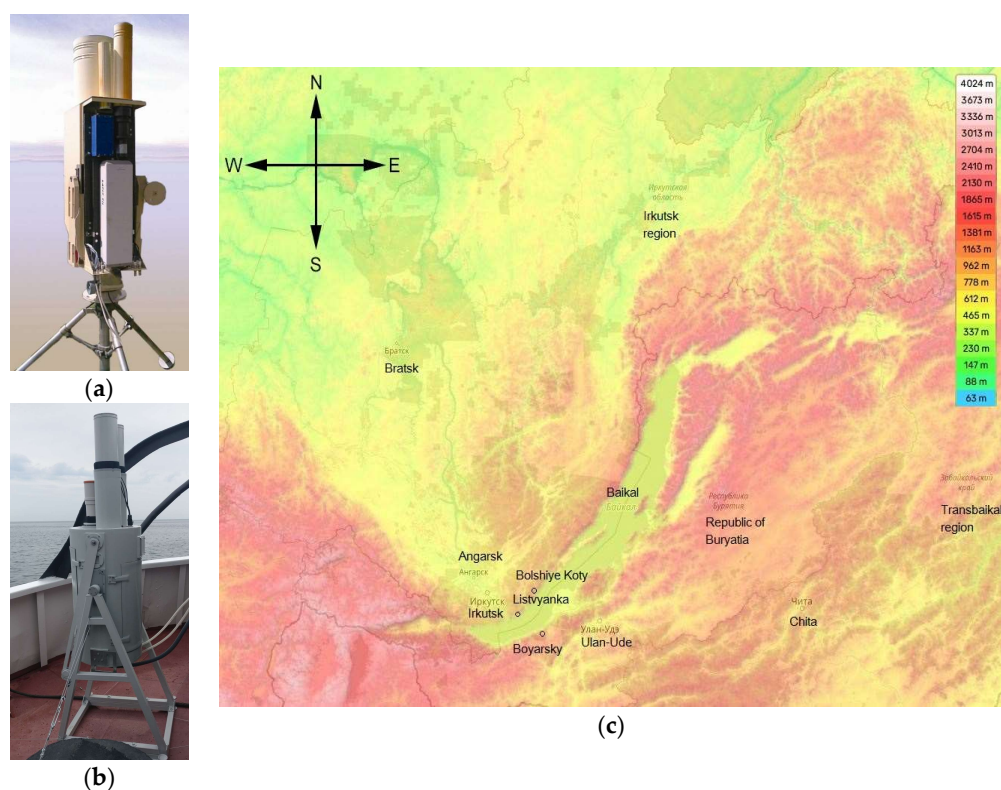


**Figure 1.** (a) Stationary LOSA-M2 and (b) shipboard LOSA-A2 lidars; (c) map of Lake Baikal.

Stationary ground-based studies have been carried out for several years with a mobile LOSA-M2 multi-frequency Raman aerosol lidar [20] in the southern part of the lake, on the eastern shore, at the Boyarsky stationary site of the Institute of Physical Materials Science, Siberian Branch, Russian Academy of Sciences (51.84°N, 106.06°E) (Figure 1c). In 2018, the mobile LOSA-A2 polarization Raman aerosol lidar [21] was specifically designed for work in difficult expeditionary conditions (Figure 1b). Complex shipboard research has been carried out since 2018 on the research vessels of the Limnological Institute, Siberian Branch, Russian Academy of Sciences, with the use of the LOSA-A2 lidar as one of the main tools for atmospheric monitoring. The route of the ship may differ in each individual expedition and is mostly determined by the weather conditions during the experiments. However, the main measurement points remain constant. Among them are: Listvyanka village, Bolshie Koty village, Olkhon Island, Severobaikalsk city, Ust-Barguzin city, the Selenga River delta, Boyarsky village, and Baikalsk city. These are the regions where the main sources of aerosol emissions are located: industrial enterprises, large power plants, popular tourist destinations, etc.

These lidars were mainly used independently in expeditionary studies at different times and in different Baikal regions. Sometimes, synchronous measurements were carried out, where one lidar was located onboard a ship, at a distance of less than 1000 m from the Boyarsky site, and the second lidar was mounted onshore. The purpose of those experiments was to study the physical processes which determine the transfer of aerosol inhomogeneities at different altitudes at the water–land interface.

Both lidars were designed according to common principles. The main requirement for them was to maintain optical settings during transportation and in difficult expeditionary conditions. Therefore, all the main components of the lidar transceivers are mounted on both sides of a single platform, which is a rigid frame. The structure is protected by a thermal and moisture-proof housing, which is also important for round-the-clock operation under different weather conditions. Nd:YAG lasers with a pulse radiation at the two wavelengths of 532 nm and 1064 nm are used as transmitters. Backscattered radiation at a wavelength of 532 nm is recorded by Hamamatsu Photonics photomultipliers (Hamamatsu City, Japan) [22] in the analog operation mode, and at a wavelength of 1064 nm, it is recorded by an original photodetector module based on a C30956E-TC avalanche photodiode (Perkin Elmer, Waltham, MA, USA) [23]. At night, a signal of spontaneous Raman scattering on atmospheric nitrogen molecules is recorded in the photon counting mode at a wavelength of 607 nm. A LOSA-A2 lidar is capable of performing polarization measurements at a wavelength of 532 nm due to the use of a Wollaston prism in the receiving part of this channel. More detailed information about the specifications and design features of the lidar systems can be found in [20,21]. Here, their main parameters are given in Table 1.

**Table 1.** Lidar parameters.

Parameter	LOSA-A2 Lidar, Shipboard Version	LOSA-M2 Lidar, Stationary Version
Transmitter		
Nd:YAG laser	LOTIS LS-2131M (Belarus)	LOTIS LS-2135 (Belarus)
Energy, mJ, at a wavelength of		
1064 nm	240	340
532 nm	120	170
Pulse duration, ns	8	10–12
Pulse repetition frequency, Hz	1–20	10
Collimator		
Beam divergence, mrad	0.2	0.5
Beam diameter, mm	50	60
Output polarization	Linear	linear
Receiver		
Receiving telescope	Two (for visible and IR regions)	Two (for near and far zones)
Telescope diameter, mm	110	50 and 250
Focal length, mm	500	200 and 1000
Field of view, mrad	1–10	1
Signal recording		
1. Receiving channel 532 nm		
Receiving mode	analog (polarized, cross-polarized)	analog (without polarization)
Detector	H11526-20-NF Hamamatsu (Hamamatsu City, Japan) [22]	H11526-20-NF Hamamatsu (Hamamatsu City, Japan) [22]
2. Receiving channel 1064 nm		
Receiving mode	analog	analog
Detector	photo module based on a C30956E-TC avalanche photodetector (IAO, Tomsk, Russia) [23]	photo module based on a C30956E-TC avalanche photodetector (IAO, Tomsk, Russia) [23]
3. Receiving channel 607 nm		
Receiving mode	photon counting (nighttime)	photon counting (nighttime)
Detector	H11706P-40-MOD Hamamatsu (Hamamatsu City, Japan) [24]	H11706P-40-MOD Hamamatsu (Hamamatsu City, Japan) [24]
Mass of the system	50 kg	60 kg

The initial interpretations of the atmospheric laser sounding data, based on the analysis of spatiotemporal 2D maps of the distribution of aerosol impurities in the atmosphere, were used in the form of color images. The optical characteristics of the aerosol were retrieved from lidar data using the well-known methods and algorithms [25,26].

The aerosol optical depth (AOD) was estimated using the method of spontaneous Raman scattering from the nighttime signals at a wavelength of 532 nm. Using the Angström power law for AOT [27], the vertical profile of the aerosol backscattering coefficient is calculated as

$$\eta_{\beta}(\lambda_1, \lambda_2, z) = \ln[\beta_{\pi}(\lambda_1, z) / \beta_{\pi}(\lambda_2, z)] / \ln[\lambda_2 / \lambda_1] \quad (1)$$

The backscattering coefficient  $\eta_{\beta}$  provides information about the effective radius of the aerosol particles and weakly depends on their volume concentration.

To measure the meteorological parameters in the surface air layer, an AMK-03 EXMETEO (SAP, Tomsk, Russia) acoustic weather station was mounted in the immediate vicinity of the LOSA-M2 lidar on the territory of the measuring site [28].

The atmospheric aerosol transfer processes were analyzed using a hybrid model of the integral Lagrangian trajectories of the particles (HYSPLIT, College Park, MD, USA) [29].

### 3. Results

#### 3.1. Observations in Background Conditions

Daily variations in the spatiotemporal structure of atmospheric aerosol over land are mainly caused by variations in the thermal conditions of the ABL [30]. Surface air layers gradually warm up during sunrise; as a result, the aerosol fills higher layers. This daily variability is one of key characteristics of the ABL and is to be taken into account in climate and ecological problems.

Changes in the ABL are relatively slow over large water bodies, such as lakes, seas, and oceans, in contrast to land. The water surface temperature changes slightly during the day because of its high heat capacity, i.e., it can absorb a large amount of solar heat under a relatively weak variation in the temperature. Thus, the slowly varying temperature of the Baikal surface has little effect on the lower part of the ABL.

Therefore, in the conditions of the Baikal mountain basin, most of the changes in the ABL above the water area are due to synoptic and mesoscale processes. When the synoptic situation is stable, daily fluctuations in the ABL over the lake can be associated with breeze circulation [31]. The daytime breeze is quite common in Baikal in summer since the lake water temperature is very low (+8 °C in July).

When studying the atmospheric aerosol in the Baikal region, it is also important to take into account the features of the topography. Due to the complex mountainous terrain around the lake, with many gorges and intermountain basins, such local winds as Sarma, Barguzin, Verkhovik, and Kultuk [11,12] are observed here; these winds cause the transport of atmospheric impurities over the water area of the lake.

The above factors are decisive in the formation of the complex vertical structure of atmospheric aerosol over Baikal and have been observed by the authors in the lidar data for several years. Figure 2 shows several examples of time–altitude sections of aerosol in the lower troposphere over Baikal; these were frequently recorded under summer background conditions in 2015–2019.

The color scale on the right side of the figures corresponds to the magnitude of the range-corrected lidar signals for the wavelength  $\lambda = 1064$  nm, where atmospheric aerosols have the strongest contribution to the light-scattering response from air. The spatial resolution is 6 m, and the temporal resolution is 1.6 s. All the figures show the results of observations from 9 to 11 am, when the processes in the atmosphere are the most dynamic due to turbulent exchange. The signal slightly changes with altitude in all the figures. The patterns are stable layered structures, where the aerosol layers are a few hundred meters thick. According to the color scale, the following altitude ranges can be distinguished: 0–400, 400–500, 500–1000, 1000–1500, and 1500–2000 m. The height of the ABL is 2500–3000 m. There is no mixing layer due to the cold water surface.

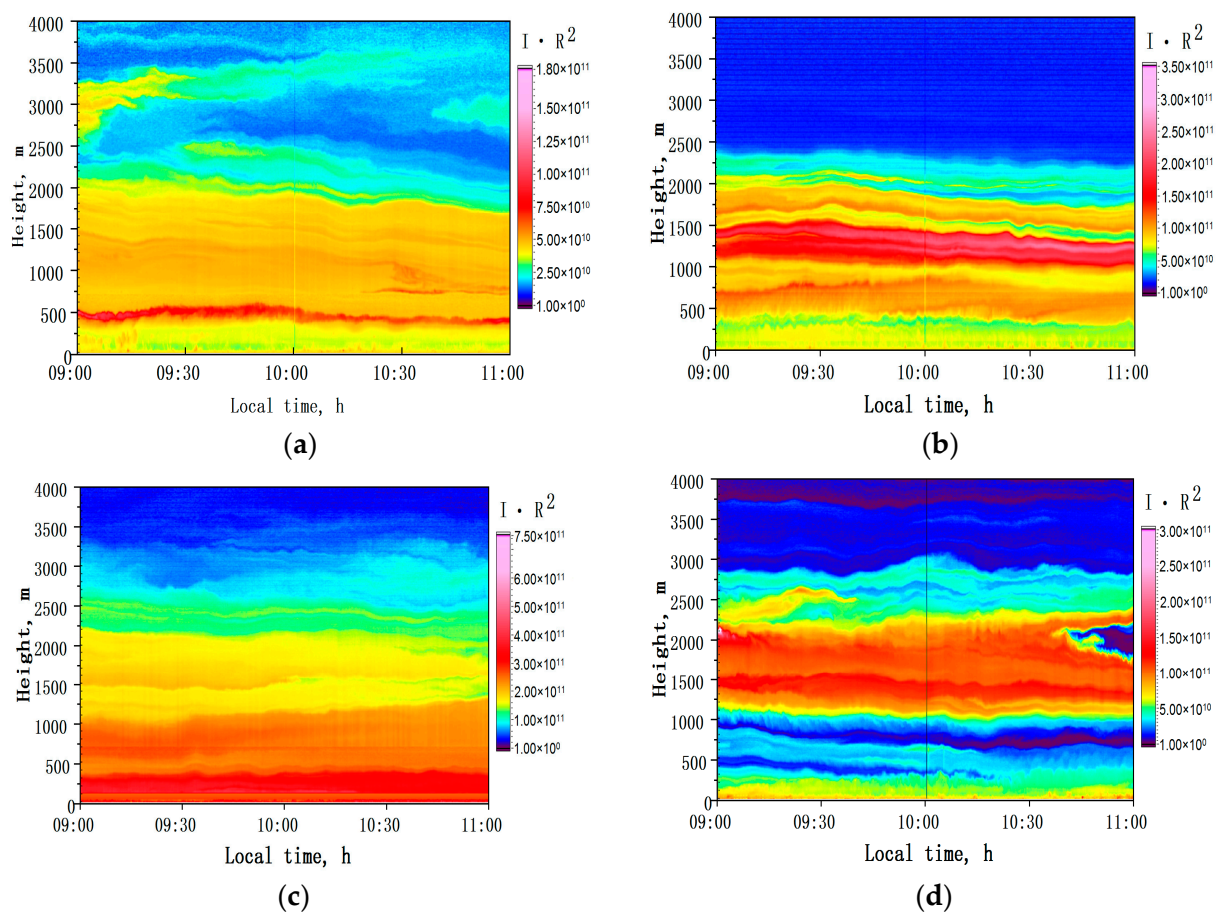


**Figure 2.** Spatiotemporal patterns of atmospheric aerosol observed with the LOSA-M2 lidar at the Boyarsky stationary site (51.84°N, 106.06°E): (a) on 3 August 2015; (b) 6 August 2016; (c) 23 July 2018; (d) 2 August 2019. Color scale—range-corrected lidar signals ( $\lambda = 1064$  nm). The vertical lines on the graphs are matched file data with a duration of 1 h.

Furthermore, for each case in Figure 2, a description of the general meteorological situation is given.

(1) 3 August 2015

On 2–3 August 2015, the territory of Baikal Lake experienced the influence of a cyclone located to the east. By 3 August 2015, Baikal Lake was on its periphery. The day before, from 1 to 2 August 2015, it rained at night, after which the background values of the aerosol content were observed. In the afternoon of 2 August 2015, cloudiness was observed at the upper boundary of the atmospheric boundary layer at 3000–3500 m. In addition, thin cirrus clouds were registered on the night of 2–3 August 2015 at an altitude of 10,000 m.

(2) 6 August 2016

At the beginning of August 2016, Baikal was influenced by two air masses. A cyclone developed to the west of the observation site, while an anticyclone was located to the south. From 3 to 4 August 2016, low cloudiness and drizzle were registered all the time, while there was light rain sometimes. On the night of 4–5 August 2016, at about 4:00 a.m., cirrus clouds appeared at 8000–10,000 m. At the same time, there was a strong near-water fog at an altitude of 200–300 m, and the measurements were suspended. On the night of 5–6 August 2016, the sky was covered with low continuous clouds, with a lower boundary at an altitude of 800–900 m. At about 6:00 a.m. on 6 August 2016, the atmosphere was clear and cloudless. A multilayer aerosol structure began to form. In the evening, at 9:00 p.m., on 6 August 2016, cirrus clouds appeared at an altitude of 9000–10,000 m.

(3) 23 July 2018

There was a cyclone to the north of the observation place. Baikal Lake was on the periphery of the cyclone on 21 July 2018; so, it rained all day and stopped on the morning of 22 July 2018. By the evening of 22 July 2018, a layer of clouds was revealed at an altitude of 5000 m. The ABL after sunset became evenly filled. On 23 July 2018, early in the morning at the upper boundary of the ABL, the remnants of former clouds were observed at an altitude of 2500–3500 m until 8 am. Then, on the morning of 23 July 2018, there were no clouds, and a layered structure appeared. By the evening of 23 July 2018, cirrus clouds appeared at an altitude of 8000–11,000 m at 8:00 p.m.

(4) 2 August 2019

It was rainy weather till 27–30 July 2019. During this period, a cyclone moved over the territory of Baikal Lake from west to east. At midnight on 1 August 2019, weak and broken cirrus clouds appeared at an altitude of 8000–11,000 m. In the afternoon of 1 August 2019, there was heavy fog at an altitude of 250 m. On this day, the atmosphere was heavily filled with smoke from forest fires up to altitudes of 5000 m. On 1 August 2019, clouds were revealed at an altitude of 3000–4000 m, while this occurred at an altitude of 2000 m from 6 am to 8:00 a.m. In the afternoon of 2 August 2019, cirrus clouds were located at an altitude of 8000–11,000 m.

Therefore, the stratification seen in Figure 2 can persist over Baikal for a long time. In [32], a good correlation was shown for lidar signals at various altitude levels in the lower troposphere at an altitude of up to 1000 m (correlation coefficient  $k \geq 0.5$ ). This indicates a single mechanism for the formation of aerosol layers in this altitude range. For an altitude above 1400 m, a negative relationship had already prevailed (correlation coefficient  $k \geq -0.5$ ). Nine fixed heights were chosen for the calculations: 400 m; 500 m; 600 m; 700 m; 1000 m; 1200 m; 1500 m; 1700 m; and 2500 m, corresponding to the positions of the lower and upper boundaries of the observed atmospheric aerosol inhomogeneities.

To determine the meteorological conditions under which the formation and transfer of the observed spatiotemporal aerosol structures happened, we used data on the altitude changes in the values of the atmospheric meteorological parameters taken from the database of the University of Wyoming [33]. This database contains information from an aerological sounding station which is the closest to the place of the lidar measurements. It is located in the city of Ust-Barguzin on the eastern shore of the lake at a distance of 260 km from the Boyarsky station. Measurements are taken twice a day, at 8:00 a.m. and 8:00 p.m. (local time). Figure 3 shows graphs of the altitude variations in the atmospheric meteorological parameters according to the measurement station in the city of Ust-Barguzin.

The boundaries of the key observed aerosol layers in the atmosphere coincided with the altitude of visible temperature inversions presented in the graphs (500 m, 1000 m, 1500 m, 2500 m, and 3000 m). Moreover, the air was more humid in the upper part of the observed aerosol layers at the altitude range of 1000–2500 m. In addition, a significant shift in the wind direction in the lower one–two kilometer layer was a characteristic feature of the considered situation. This was obviously due to the orography of the area. Below the indicated range of heights, local wind currents predominate, while westward transport was already in effect at the above altitudes.

The main problem is the insufficient density of aerological stations on the territory of Baikal Lake; so, this makes it difficult to conduct a deeper analysis. Additional measurements of the atmospheric meteorological parameters directly above the lidar location during the experiments are required. In addition, balloon-probe measurements cannot detect temperature microinversions in the atmosphere (with a length of several meters or several tens of meters).

Another feature pronounced in the lidar data, which can be associated with the temperature and wind regimes of the lake basin, is the daily variation in the altitudes of the aerosol layers in the atmosphere over Baikal, including the maximal filling altitude. That is, the aerosol does not rise from the ABL to higher layers as the air is warming up in daytime.

On the contrary, due to a change in the wind direction, the aerosol gradually descends to the ground under the action of breeze circulation (Figure 4). Cold air coming from the lake does not allow the aerosol to rise higher. The intensity of turbulent mixing decreases. The speed of aerosol descent is  $\sim 100\text{--}200$  m/h at different altitudes.

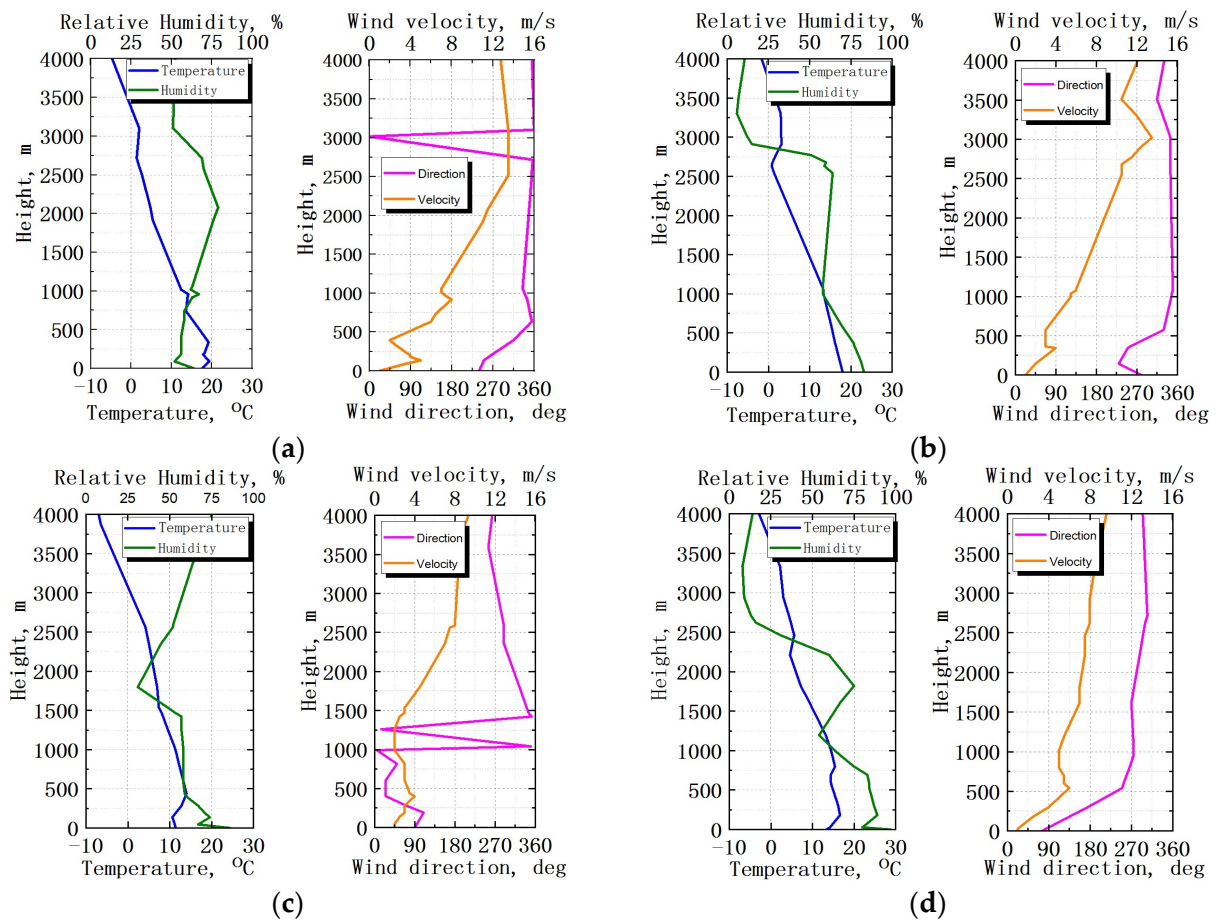


**Figure 3.** Altitude variations in atmospheric meteorological parameters [33]: (a) 8:00 a.m., 3 August 2015; (b) 8:00 a.m., 6 August 2016; (c) 8:00 a.m., 23 July 2018; (d) 8:00 a.m., 2 August 2019.

Furthermore, for each case in Figure 4, a description of the general meteorological situation is given.

(1) 8 August 2016

On the eve of the moment of the lidar observations, a cyclone moved over the region to the east. On 7 August 2016, it began to rain in the evening. On 8–9 August 2016, according to the data, no large air masses were observed over the Baikal territory. On the morning of 8 August 2016, at 11:00 a.m., the measurements were resumed. There was a heavy fog at an altitude of 200 m. There were no clouds. Very weak cirrus clouds appeared in the afternoon at an altitude of 8000 m. By evening, the cloudiness lowered to an altitude of 4000 m. On the night of 8 August 2016, another layer of cirrus clouds appeared at an altitude of 10,000–11,000 m.

(2) 5 August 2017

To the south of Baikal Lake, there was a cyclone that moved from west to east. On 2 August 2017, it began to rain in the afternoon. On 4 August 2017, cirrus clouds were observed all day long at an altitude of 8000–11,000 m and by the evening of 4 August 2017. Until 11:00 a.m. on 5 August 2017, there were small clouds at an altitude of 2500–4000 m.

In the afternoon, the atmosphere was cloudless, while separate faint clouds appeared only by 20:00 on 5 August 2017 at an altitude of 10,000 m.

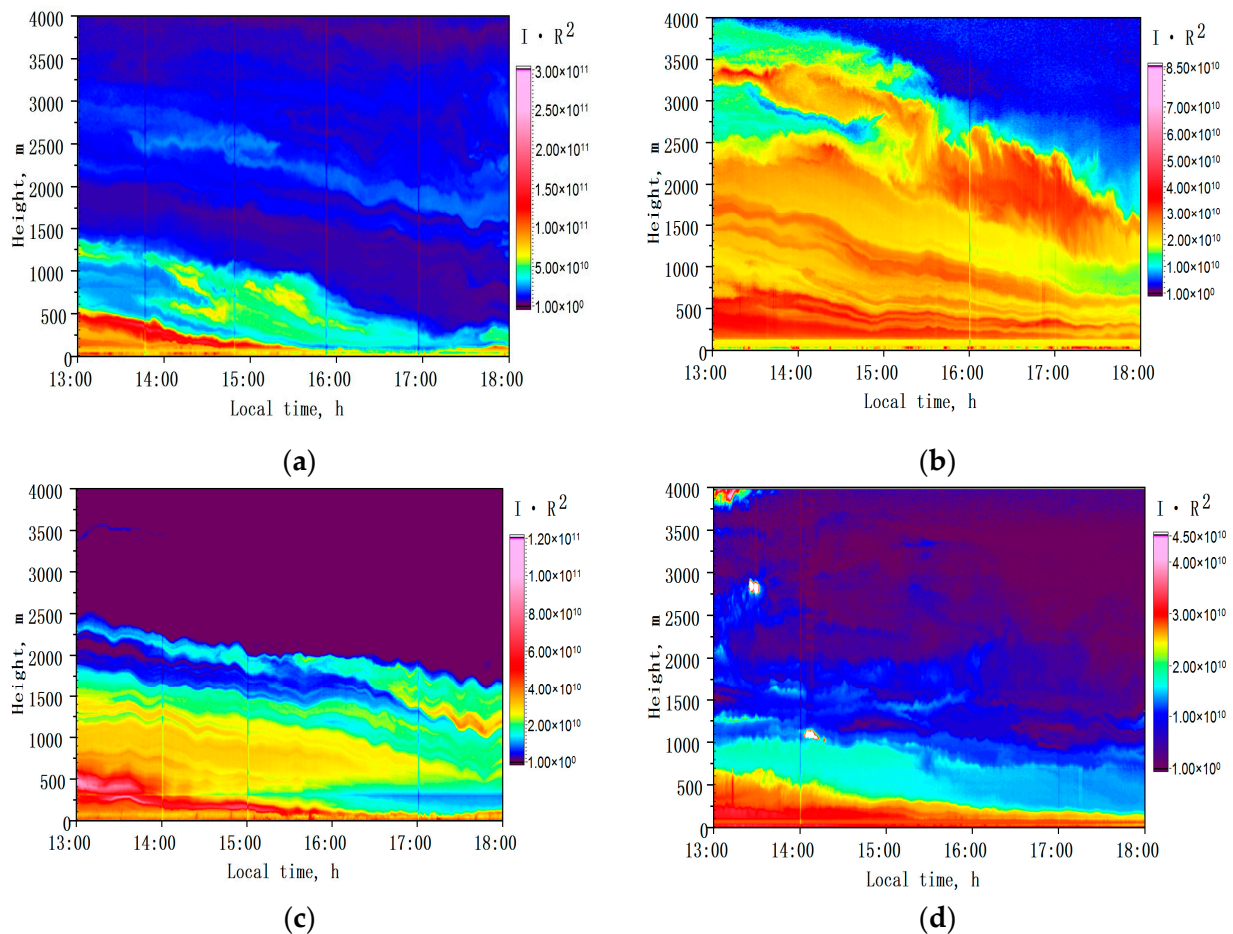


**Figure 4.** Spatiotemporal patterns of atmospheric aerosol observed with the LOSA-M2 lidar at the Boyarsky stationary site (51.84°N, 106.06°E): (a) on 8 August 2016; (b) 5 August 2017; (c) 8 August 2017; (d) 18 July 2018. Color scale—range-corrected lidar signals ( $\lambda = 1064$  nm). The vertical lines on the graphs are matched file data with a duration of 1 h.

### (3) 8 August 2017

On the night of 7 August 2017, at 1:00 a.m., clouds appeared at an altitude of 4000 m and gradually gained strength, and it began to rain by 4:00 a.m. on 7 August 2017. For this reason, the measurements had to be suspended. We continued them on the night of 7–8 August 2017, when the clouds were located at an altitude of 3500–4000 m; they disappeared by 8:00 a.m. in the morning. Cirrus clouds had already appeared at an altitude of 10,000–11,000 m by 9:00 a.m.

### (4) 18 July 2018

As in most of the cases described above, a cyclone operated to the west of Baikal Lake and moved eastward. At 11:00 p.m. on 17 July 2018, it rained. On the morning of 18 July 2018, there was heavy fog and multi-layered clouds at altitudes of 1500 m, 2500, and 4000 m. After 2:00 p.m., no clouds were evident.

The analysis of the weather data from the AMK-03 “EXMETEO” acoustic weather station, located on the Boyarsky site in the immediate vicinity of the LOSA-M2 lidar, for the period from 2010 to 2022 showed a change in the wind direction during the day. From the set of meteorological data for that long-term period, we selected only the data for the time periods when the lidar observations were carried out. Figure 5 shows the daily variation in

the wind direction in the surface air layer. Each point was derived by averaging over an hour. According to the results, the wind direction gradually changed from  $220^\circ$  (along the coast) to  $270^\circ$  (from the lake) during the daytime.

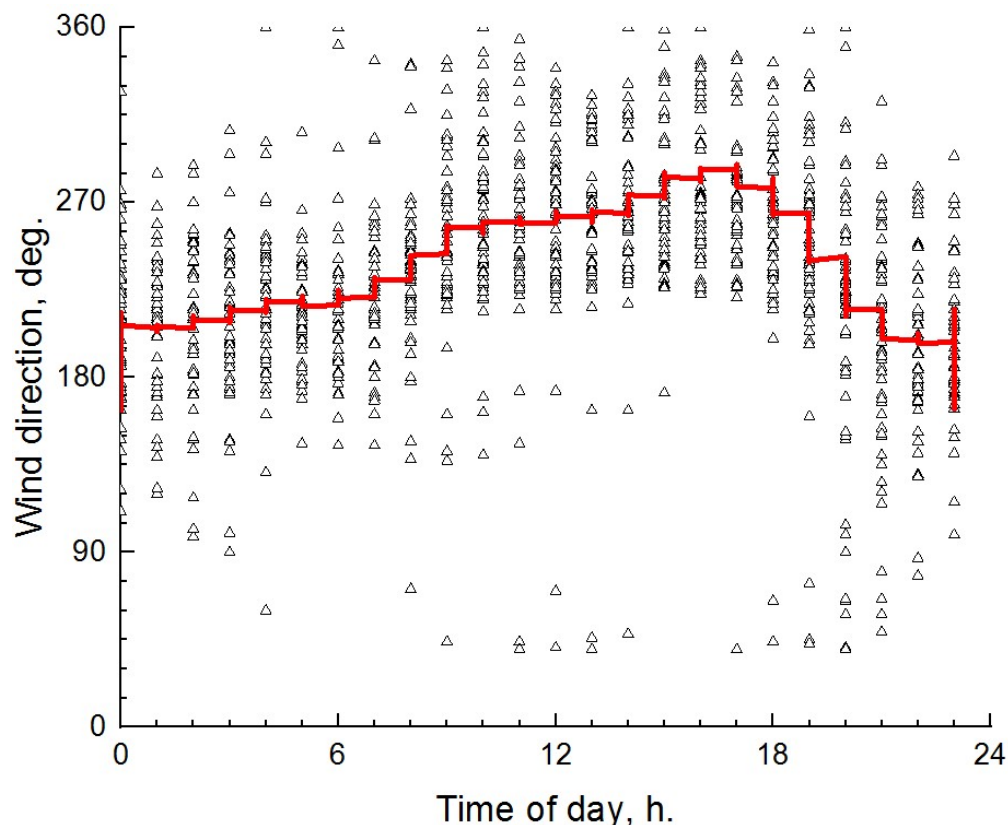


**Figure 5.** Daily variations in the wind direction according to observations at Boyarsky site; the red curve shows the average values. Each point (triangle) was derived by averaging over an hour.

Thus, the meteorological data considered confirm the decisive effect of breeze circulation on the formation of atmospheric aerosol over Baikal in the daytime in summer.

### 3.2. Observations under Wildfire Conditions

The results of the annual complex ship expeditions on Lake Baikal aimed at air pollution monitoring reliably show an increase in the content of gas and aerosol impurities in the air in recent years as a result of large-scale wildfires in the Irkutsk region, the Republic of Buryatia, Krasnoyarsk Territory, and the Republic of Sakha Yakutia [6,7].

As smoke aerosol is a good tracer, lidars allow the tracing of the transport of atmospheric aerosol impurities that fill the atmosphere in the mountainous surroundings. As an example, Figure 6 shows two different situations with smoke plumes from wildfires with the sources located at different distances from the observation site.

Figure 6a shows the case of a powerful aerosol plume from wildfires in the Krasnoyarsk Territory and Yakutia, which are far from Lake Baikal. This is confirmed by satellite monitoring data [34] and the trajectory analysis performed with the HYSPLIT model [29] (Figure 6b). The smoke plume was observed while the ship was moored near the town of Severobaikalsk, in the northern part of the lake. Note that the Baikal Mountains, the prevailing heights of which are 1900–2200 m, extend to the west of the experiment location. The night before, 21 July 2018, it rained, and the ABL was cleared. On the night of 22–23 July 2018, at approximately 1:00 a.m., smoke aerosol appeared in the form of two separate layers 200–300 m thick at the height of the observed clouds (Figure 6a).

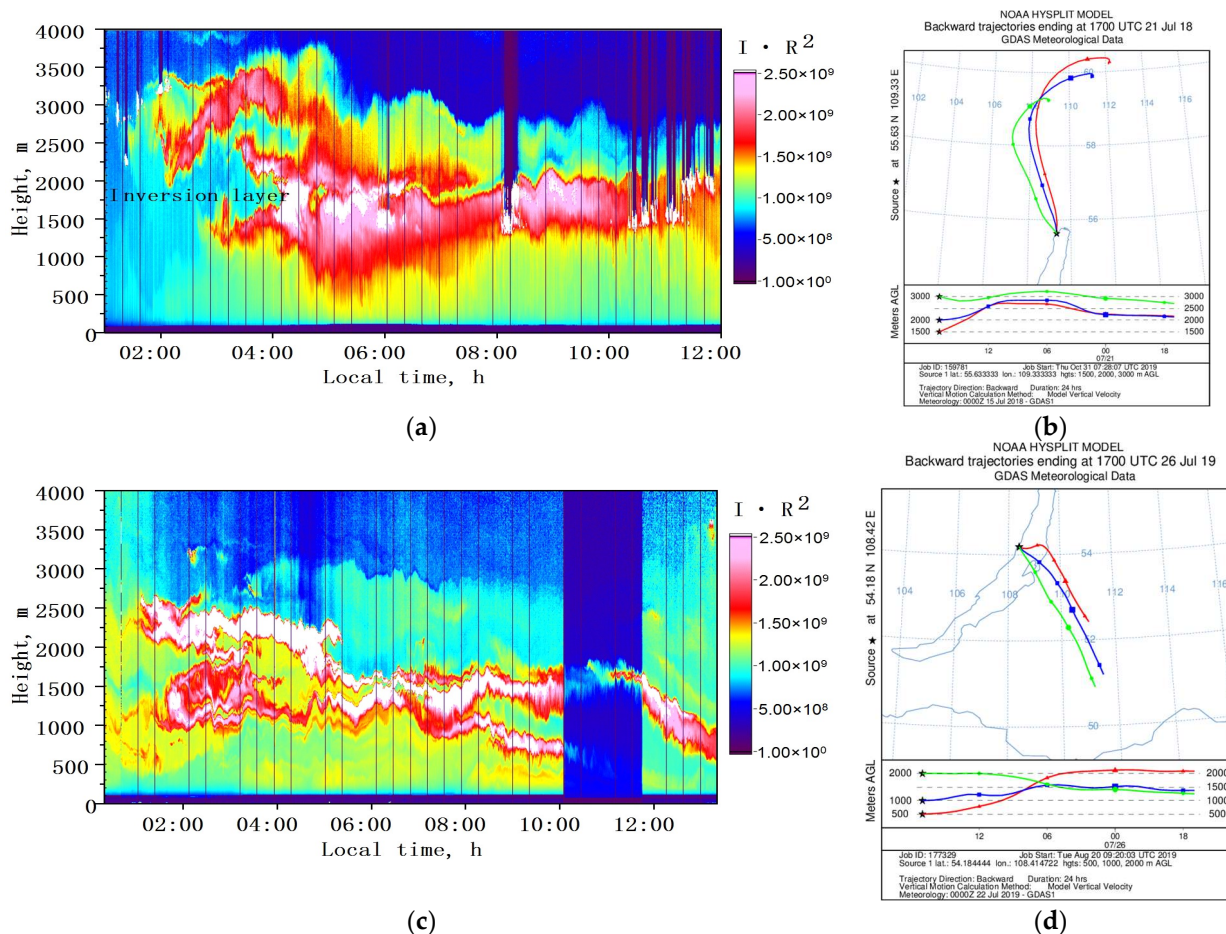


**Figure 6.** Spatiotemporal structures of aerosol in the troposphere observed with the LOSA-A2 lidar during ship expeditions: (a) on 22 July 2018 and (c) 27 July 2019; (b,d) back trajectories calculated using the HYSPLIT model [29] for these two cases, respectively. Color scale—range-corrected lidar signals ( $\lambda = 532$  nm). There is a gap in data on 27 July 2019, from approximately 10:00 to 12:00, caused by a failure in the system synchronization. The vertical lines on the graphs are matched file data with a duration of 20 min. The star symbol on (b,c) indicates the place of measurements.

Later, at 2:30 am, another layer appeared at an altitude of 1500 m (Figure 7a). All three layers exhibited the same depolarization ( $\sim 5\%$ ). The layers expanded gradually in the vertical direction. The introduced layers of smoke were obviously warmer than the surrounding air above the observation point; this was the reason for their rising. At the same time, the observations showed that an aerosol at 1500 m could not exceed a height of 2000 m, where the temperature inversion layer was probably located. A characteristic feature of the measurements carried out was that the temperature inversion at a height of 2000 m persisted throughout the entire observation period. Below the inversion layer, condensation sometimes occurred on the smoke aerosol particles and a weak cloudiness formed (the degree of depolarization increased up to 10% due to multiple scattering on the watered particles). Larger aerosol particles in the lower layer gradually began to sediment (Figure 7b). In the morning, the lower boundary of the aerosol plumes got down below 1000 m. The set of gas–aerosol equipment located directly on the ship did not register any significant excesses of soot or gas impurities.

Figure 6c shows the case of a “short-range” transported smoke plume. By about 01:00 on 27 July 2019, two aerosol plumes were observed at altitudes of 1500–1500 and 2000–2500 m, with approximately the same depolarization (Figure 7c). The ship passed northward along the western shore of the lake at that time and stopped near Elokhin Cape (from 4:00 to 11:24 on 27 July 2019). In that case, according to the satellite data for 26 July

2019, a wildfire's focus was on the eastern shore opposite the ship's mooring point, near Sosnovka Bay. The back trajectory analysis (Figure 6d) showed that the smoke from the wildfire was spreading northwestward over the lake by the time the ship passed along the western shore. As can be seen from Figure 7c,d, the smoke aerosol gradually descended into the underlying layers. By the morning, the lower layer at 750 m was more strongly depolarized, which indicated the presence of larger aerosol particles in the layer. At the same time, the two-layer structure of the aerosol in the atmosphere was kept.

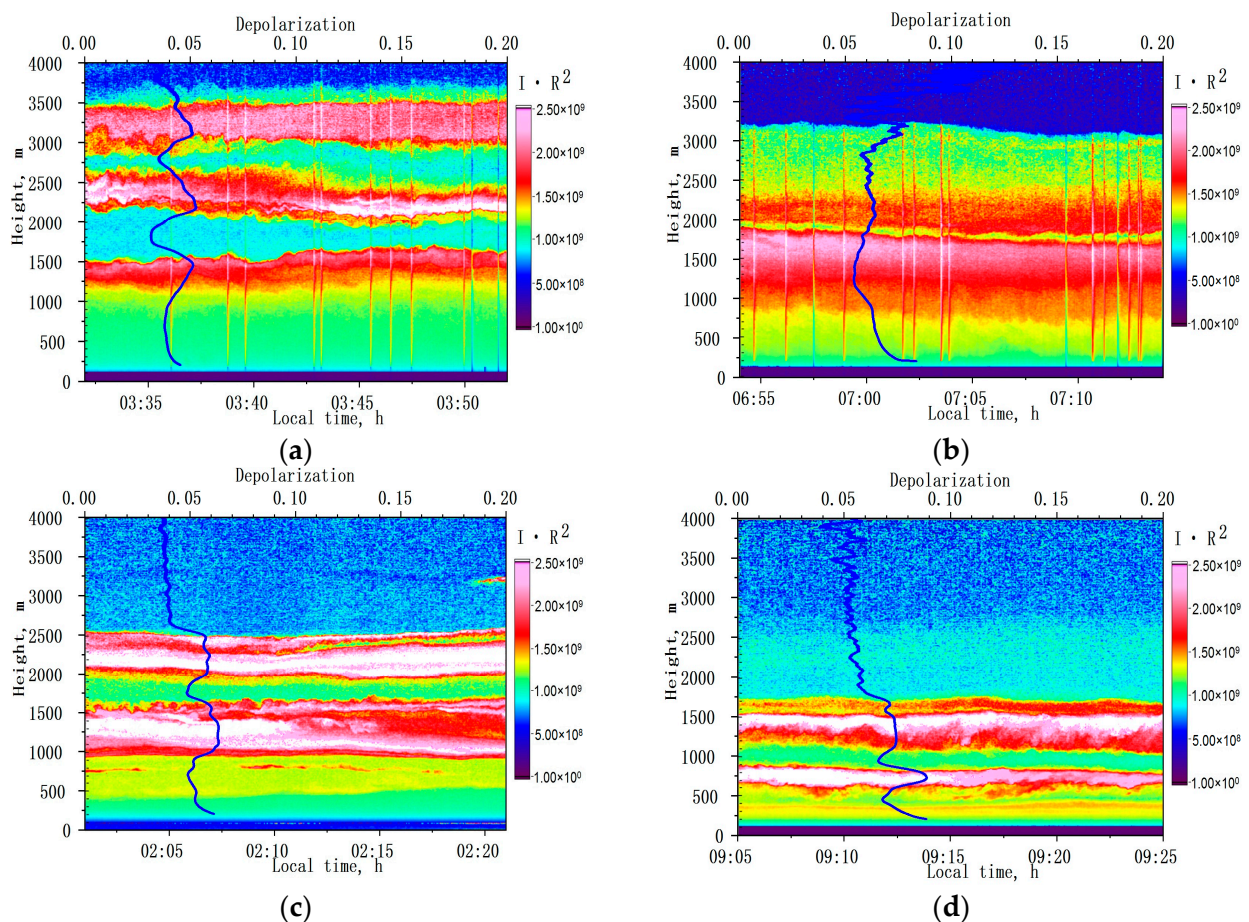


**Figure 7.** Spatiotemporal structures of aerosol in the troposphere observed with the LOSA-A2 lidar at a radiation wavelength of  $\lambda = 532$  nm during ship expeditions, and the vertical profile of the degree of depolarization (blue lines) at night and in the morning: (a,b) on 22 July 2018 and (c,d) on 27 July 2019. Color scale—range-corrected lidar signals ( $\lambda = 532$  nm).

### 3.3. Calculations of AOD and Angström Parameter

In addition to studying the spatiotemporal characteristics of aerosols in the mountain basin, we calculated the optical and microphysical parameters of the atmosphere under different observation conditions (background and extreme situations associated with wildfires) on the basis of long-term lidar observations in summer, including the optical characteristics of the smoke aerosol brought to Lake Baikal from wildfires at different distances from the observation site.

In [35], the authors revealed a trend towards an increase in AOD by 0.013 per year based on the analysis of photometric observations at Lake Baikal from 2010 to 2020. The maximal turbidity of the atmosphere was observed in the period from 2018 to 2020, when the AOD varied from 0.22 to 0.27. Strong wildfires occurred in Siberia during those years.

Figure 8 shows two cases of lidar observations at Lake Baikal in 2019 during the most extreme atmospheric situations associated with strong wildfires.

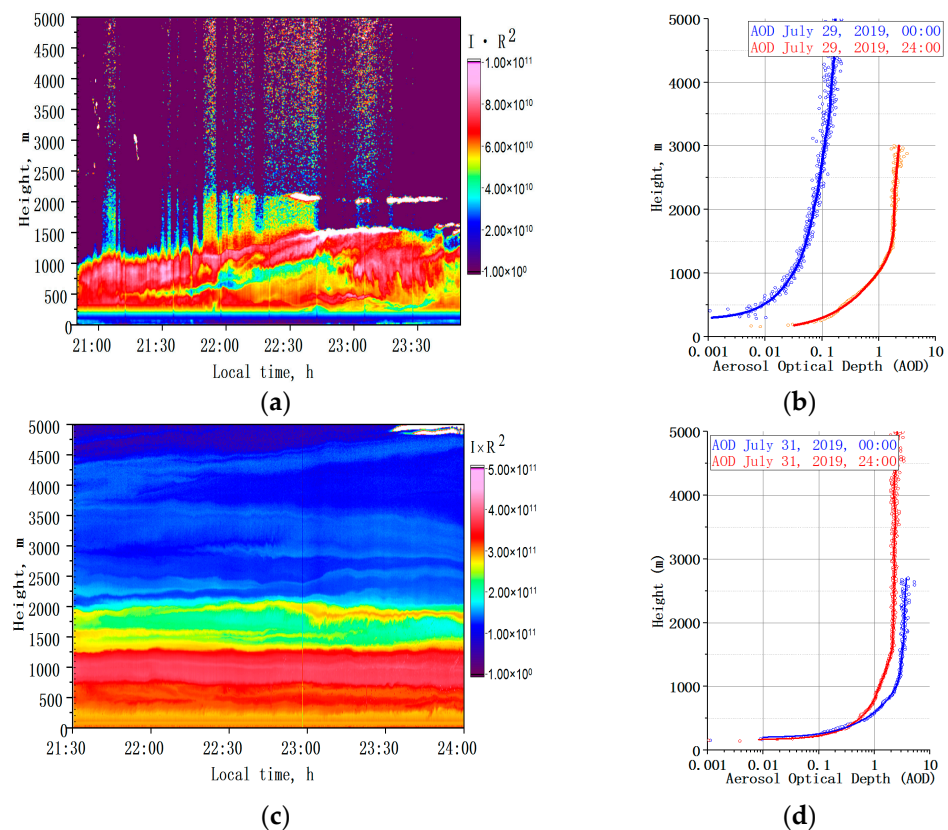


**Figure 8.** Spatiotemporal patterns of aerosol in the troposphere according to data of: (a) shipboard LOSA-A2 lidar on 29 July 2019 and (c) stationary LOSA-M2 lidar on 30 July 2019. AOD profiles at  $\lambda = 532$  nm on 29 July 2019: (b) at 00:00 (blue line) and at 24:00 (red line). AOD profiles at  $\lambda = 532$  nm on 31 July 2019: (d) at 00:00 (blue line) and at 24:00 (red line). The vertical lines on the graphs are matched file data with a duration of 20 min for lidar LOSA-A2 (a) and 1 h for lidar LOSA-M2 (c).

Figure 8a shows an example of the vertical section of an aerosol in the troposphere on 29 July 2019, derived from the data of the LOSA-A2 lidar mounted on board a ship moving in the northeastern part of Baikal. One can see the appearance of a smoke plume, which was transported from the north with anticyclonic air masses and filled the ABL above Baikal up to 2000 m. The spatial structure of this aerosol plume was obviously complex and was broken at the beginning of its entry into the lake basin.

Figure 8b shows a vertical section of an aerosol on 30 July 2019, derived from data of the LOSA-M2 lidar located further south at the Boyarsky stationary site. As can be seen, a day later, on the night of 31 July, the smoke plume reached the southeastern shore of Lake Baikal and homogeneously filled the ABL up to an altitude of 2000 m.

The AOD profiles are shown on the right. The main contribution to the AOD of the smoke plume was made by the aerosol contained inside the ABL within 2000 m. The AOD in this layer was  $\tau \approx 1.6$  on July 29, and it attained  $\sim 4$  on 30 July. The latter value was obtained under the threshold conditions of the lidar operation when photodetectors were overloaded due to high-power lidar signals from the dense aerosol formations and the experiment had to be stopped.

Table 2 shows the Angström parameter and AOD calculated for different atmospheric conditions (background; smoke plumes transported to the atmosphere over the lake from different regions) and averaged over the ABL.

The conditions on 2 August 2015 were considered as a typical background situation for Lake Baikal in summer. The AOD value was equal to 0.09, which corresponded to the observation period average values obtained by photometric methods in warm seasons [35].

**Table 2.** ABL average values of the Angström parameter for different atmospheric conditions.

Date	Altitude Range, m	Angström Parameter	AOD
Clear air			
2 August 2015	150–2500	$1.57 \pm 0.16$	0.09
9 September 2021	150–12,000	$1.58 \pm 0.15$	0.10
Short-range smoke transport			
3 August 2015	150–3000	$1.05 \pm 0.08$	0.25
Long-term smoke transport			
14 August 2015	150–3750	$1.13 \pm 0.12$	0.26
Far-range smoke transport			
7 August 2013	150–2250	$1.41 \pm 0.07$	0.64

In the situation of “long-range smoke transfer” (7 August 2013), the Angström parameter overlapped with the background value for 2 August 2015, within the standard deviation, which indicated the homogeneous particle size distribution of the aerosol, although the AOD differed by  $\sim 7$  times. The fine aerosol fraction dominates in the size distribution of aerosol particles in these atmospheric situations. The only difference in the case of the long-range transport of smoke aerosol is that the aerosol particles are finer and their distribution is shifted towards larger sizes. These aerosol particles were transported to Lake Baikal from large-scale wildfires in the forest tundra of Yakutia in July–August 2013. By the morning of 7 August, with a northern cyclone, air masses with maximal concentrations of smoke aerosol reached the lidar observation site in southern Baikal. The trajectory analysis showed that the aerosol was transported by air masses to 1500–2000 m in 4–5 days.

The particle size distributions of the smoke aerosol from the wildfires in the coastal area of Lake Baikal were similar in the atmospheric situations of “short-range smoke transport” (3 August 2015) and “long-term smoke transport” (14 August 2015). This follows from the equal median values of the Angström parameter on 3 and 14 August 2015, which were retrieved from measurements under these conditions, with equal standard deviations. The values of the Angström parameter indicated the presence of the coarse fraction in the particle size spectrum of the smoke aerosol. The vertical profiles of the Angström parameter showed similar trends in these situations: the aerosol particles showed a layer-by-layer decrease in size from the surface layer, where the largest particles were detected, to the free atmosphere, where the aerosol particles were finer. This trend was kept, though the spatiotemporal structure of the aerosol in the troposphere was layered in this period, with different aerosol densities in the layers.

The similarity of the vertical profiles of the Angstrom parameter and of the aerosol particle size distributions under different atmospheric conditions in August 2015 was due to the common origin of the smoke aerosol, that is, the emission from burnt coniferous forests in the coastal areas of Lake Baikal. In August 2013, the smoke aerosol was emitted by burnt forest tundra in the Yakutia region.

#### 4. Discussion

A general analysis of the meteorological situation in the area of Lake Baikal was carried out using several open sources. The analysis of the synoptic situation was carried out on the basis of the data of the Federal State Budgetary Institution “Arctic and Antarctic Research Institute” (Russia) [36]. The data on the altitude changes in the values of the meteorological parameters of the atmosphere were taken from the database of the University of Wyoming (USA) [33]. Also, when studying the processes of atmospheric aerosol transfer, backward trajectories were calculated using the hybrid single-particle Lagrangian integrated trajectory model (NOAA HYSPLIT, College Park, MD, USA) [29].

Thus, it can be concluded that for almost all the observation cases presented in Figures 2 and 4 the general synoptic situation was similar. The layered structure of the aerosol in the atmosphere was observed when Baikal Lake was located on the periphery of a cyclonic air mass that passed over the region the day before, bringing rainy and cloudy weather. The atmosphere was cleansed by the passing rains. Then, there came the gradual filling of the ABL with aerosol due to regional and local sources. Due to the relatively cold surface of the lake, there was no noticeable turbulent mixing of the aerosol in the atmosphere, due to which the aerosol layers at different heights retained their structure for a long time.

To be noted is the appearance of cirrus clouds in the moments before and after the aerosol structures, as can be seen in Figures 2 and 4. Cirrus clouds are almost always observed in cyclones and thus can be a criterion for predicting the appearance of a layered aerosol structure in the atmosphere over Baikal Lake.

However, as the long-term lidar observations on Lake Baikal show, the global model for predicting changes in atmospheric meteorological parameters under the conditions of the Baikal basin is poorly applicable and provides only a qualitative idea of the synoptic situation on the scale of the entire region. This is primarily due to the fact that such models do not take into account the specific features of the wind regime in the mountain basin, due to the complex orography of the area. For more accurate forecasting of environmental and climatic changes in this region, it is necessary to have more information about the nature of the local air currents and the processes of interaction between the atmosphere and the cold underlying surface of the lake.

As was shown by the authors of [13], according to the results of aircraft observations over Baikal, the effect of internal hollow air circulation was discovered. This effect is not associated with the main western transport and is manifested in the movement of air along the western coast from north to south and along the eastern coast from south to north. The vertical length of such circulation cells is 1400 m (Figure 9). The lower boundary is located at a height of 300 m, and the center of the cell is located in an area of 800 m. The basin circulation in Baikal is quite stable over time.

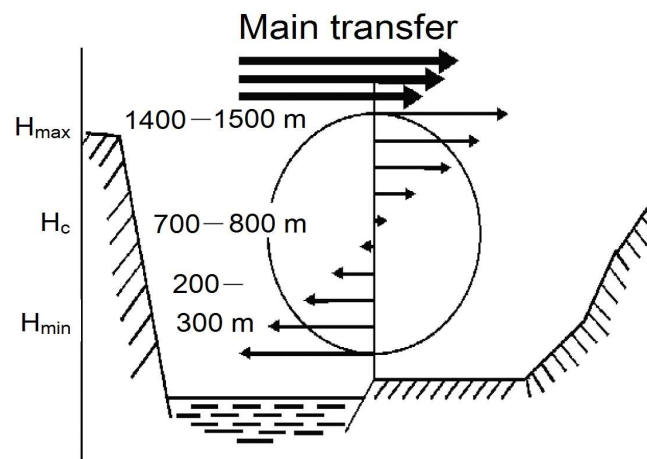


Figure 9. Wind circulation cell model [32].

A physical process similar to that of the internal basin circulation is the action of the breeze circulation. According to [31], the vertical scales of the breeze cells are determined as follows: up to 600 m, the direction of transfer from the lake to land; from 700 m to 1000 m, the transition layer, where the transfer can be equally probable in both directions; and above 1100 m, where the direction of transfer changes to the opposite direction, from land to the lake. The two main mechanisms described above determine the transport of aerosol layers in the altitude range of 0–1500 m.

Above 1500–2000 m, the main western transport begins to operate, and the aerosol layers may be the result of transport from neighboring regions. In addition, a possible mechanism for the appearance of aerosols at these altitudes is the inversion distribution of atmospheric temperature, followed by the filling with aerosols under inversion. In particular, such filling at altitudes of 2000–2500 m often leads to the appearance of cloud formations.

The paper also shows the results of observations under wildfire conditions. Figures 6 and 7 show two different situations with smoke plumes from wildfires, with the sources located at different distances from the observation site. Similar patterns of aerosol distribution, obtained on the basis of lidar data, once again confirm the complex processes of formation and transport of atmospheric aerosols in the conditions of a mountain basin. Due to the cold water surface, the aerosol often does not rise to the overlying layers as it warms up during the day into the overlying layers.

## 5. Conclusions

The high spatial resolution of the mobile ground-based lidars used in our experiments allowed the study of the finer spatial structure of aerosols over Baikal, which cannot be determined from, for example, photometric measurements or satellite lidar observations. The long-term ground-based lidar measurements over the period from 2010 to 2022 showed the complex vertical structure of aerosols in background summer conditions, with the layered distribution of the aerosol content in the altitude range of 0–2000 m. The following ranges were distinguishable in the altitude stratification: 0–400, 400–500, 1000–1500, and 1500–2000 m. The ABL height was 2500–3000 m. Because of the high temperature contrast between the Baikal water surface and the land, the aerosol does not rise to high layers under the action of convective currents. Therefore, the layer structure persists for a long time, and aerosol layers are usually “pressed down” by cold air from the lake and descend to the ground at a rate of 100–200 m/h in the afternoon due to the breeze circulation.

We studied the transport of aerosols in the Baikal mountain basin in the cases when Siberian wildfires were the main source of smoke aerosol. Smoke aerosol plumes enter into the mountain basin and become part of a complex altitude–time structure due to the topography features and under the action of local winds. The smoke impurities gradually settle on the lake surface and thus pollute it.

The complex spatiotemporal structure of atmospheric aerosols over Baikal confirms a need to consider the local features associated with the mountain surroundings and the temperature and wind conditions when predicting climate and environmental changes in the region for more reliable results. To do this, it is necessary to have a more developed network of stations for high-altitude measurements of atmospheric meteorological parameters and lidar measurements; this network is currently poor.

We estimated the optical characteristics of the smoke aerosol brought to Lake Baikal from the wildfires which take place at different distances from the observation site. The difference was shown between the microstructure of the smoke aerosol plumes from the local wildfires within the coastal area of the lake and that from distant wildfires.

The Angström parameter and the aerosol optical depth were calculated for different atmospheric conditions:  $\eta_{\beta} = 1.57 \pm 0.16$  and  $\tau = 0.09$  under background conditions;  $\eta_{\beta} = 1.41 \pm 0.07$  and  $\tau = 0.64$  for the case of smoke aerosol from distant wildfires; and  $\eta_{\beta} = 1.05 \pm 0.08$  and  $\tau = 0.25$  for the case of smoke aerosol from local wildfires.

**Author Contributions:** S.N., investigation, formal analysis, writing—original draft; Y.B., conceptualization, methodology, writing—reviewing and editing; M.K., investigation, formal analysis; G.K., methodology, investigation, formal analysis; M.N., software, validation, data curation; I.P., methodology, investigation, formal analysis. All authors have read and agreed to the published version of the manuscript.

**Funding:** The analyses of long-term lidar data were supported by the Russian Science Foundation project no. 22-77-10043, <https://rscf.ru/en/project/22-77-10043/> (accessed on 27 July 2023).

**Data Availability Statement:** Images of spatial sections of atmospheric aerosol of Lake Baikal received during the annual lidar expeditions and meteorological data during the observations can be seen on the website of the Institute of Atmospheric Optics, Siberian Branch, Russian Academy of Sciences (<http://loza.iao.ru/Data/baikal/>, accessed on 20 May 2023).

**Acknowledgments:** The expeditions employed the equipment and research vessels of the Limnological Institute of the Siberian Branch of the Russian Academy of Sciences (Irkutsk, Russia), as well as the equipment and material and technical facilities of the Boyarsky Station, the Institute of Physical Materials Science of the Siberian Branch of the Russian Academy of Sciences (Ulan-Ude, Russia). The authors express their gratitude to the staff of these institutes for their help in organizing and conducting research on Baikal Lake.

**Conflicts of Interest:** The authors declare no conflict of interest.

## References

1. Golobokova, L.; Khodzher, T.; Obolkin, V.; Potemkin, V.; Khuriganova, O.; Onischuk, N. Aerosol in the atmosphere of the Baikal region: History and contemporary researches. *Limnol. Freshw. Biol.* **2018**, *1*, 49–57. [[CrossRef](#)]
2. Panchenko, M.V.; Domysheva, V.M.; Pestunov, D.A.; Sakirko, M.V.; Shamrin, A.M.; Shmargunov, V.P. Carbon dioxide in the atmosphere-water system and biogenic elements in the littoral zone of Lake Baikal during period 2004–2018. *J. Great Lakes Res.* **2020**, *46*, 85–94. [[CrossRef](#)]
3. Obolkin, V.A.; Potemkin, V.L.; Makukhin, V.L.; Khodzher, T.V.; Chipanina, E.V. Long-range transport of plumes of atmospheric emissions from regional coal power plants to the south Baikal water basin. *Atmos. Ocean. Opt.* **2017**, *30*, 360–365. [[CrossRef](#)]
4. Banakh, V.A.; Smalikho, I.N. Lidar observations of atmospheric internal waves in the boundary layer of the atmosphere on the coast of Lake Baikal. *Atmos. Meas. Tech.* **2016**, *9*, 5239–5248. [[CrossRef](#)]
5. Zayakhanov, A.S.; Zhamsueva, G.S.; Sungrapova, I.P.; Tsydygov, V.V. Features of diurnal variability of ultrafine aerosol in the air of the Baikal coastal zone and arid zone of Mongolia. *Atmos. Ocean. Opt.* **2018**, *31*, 257–262. [[CrossRef](#)]
6. Popovicheva, O.; Molozhnikova, E.; Nasonov, S.; Potemkin, V.; Penner, I.; Klemasheva, M.; Marinaite, I.; Golobokova, L.; Vratolis, S.; Eleftheriadis, K.; et al. Industrial and wildfire aerosol pollution over world heritage Lake Baikal. *J. Environ. Sci.* **2021**, *107*, 49–64. [[CrossRef](#)] [[PubMed](#)]
7. Zhamsueva, G.; Zayakhanov, A.; Tsydygov, V.; Dementeva, A.; Balzhanov, T. Spatial-temporal variability of small gas impurities over lake Baikal during the forest fires in the summer of 2019. *Atmosphere* **2021**, *12*, 20. [[CrossRef](#)]
8. Tashchilin, M.; Yakovleva, I.; Sakerin, S.; Zorkaltseva, O.; Tatarnikov, A.; Scheglova, E. Spatiotemporal variations of aerosol optical depth in the atmosphere over Baikal region based on MODIS data. *Atmosphere* **2021**, *12*, 1706. [[CrossRef](#)]
9. Domysheva, V.M.; Panchenko, M.V.; Pestunov, D.A.; Sakirko, M.V.; Shamrin, A.M. Estimation of primary production in the water of the coastal zone of Lake Baikal based on daily variations in CO<sub>2</sub> concentration in different seasons of 2005–2021. *Atmos. Ocean. Opt.* **2023**, *36*, 92–100. [[CrossRef](#)]
10. Pyanova, E.A.; Penenko, V.V.; Gochakov, A.V.; Faleychik, L.M. Modeling the propagation of impurities from point sources in the winter atmosphere of the Baikal region. *Proc. SPIE Intern. Soc. Opt. Eng.* **2020**, *11560*, 1156071. [[CrossRef](#)]
11. Shamsheva, T.V. Wind regime over Baikal. *Collect. Irkutsk. GMO Name A.V. Voznesensk.* **1967**, *2*, 52–80. (In Russian)
12. Berkin, N.S.; Makarov, A.A.; Rusinek, O.T. *Baikal Studies*; State University Press: Irkutsk, Russia, 2009; pp. 76–85. (In Russian)
13. Arshinov, M.Y.; Belan, B.D.; Ivlev, G.A.; Rasskazhchikova, T.M. Spatiotemporal characteristics of air circulation in the hollow of Lake Baikal. *Atmos. Ocean. Opt.* **2001**, *14*, 263–266. (In Russian)
14. UNESCO. World Heritage Convention. Available online: <https://whc.unesco.org/ru/list/754>. (accessed on 22 May 2023).
15. Van Malderen, H.; Van Grieken, R.; Khodzher, T.; Obolkin, V.; Potemkin, V. Composition of individual aerosol particles above Lake Baikal, Siberia. *Atmos. Environ.* **1996**, *30*, 1453–1465. [[CrossRef](#)]
16. Zhamsueva, G.S.; Khodzher, T.V.; Balin, Y.S.; Zayakhanov, A.S.; Tsydygov, V.V.; Penner, I.E.; Nasonov, S.V.; Marinayte, I.I. Experimental studies of aerosol and gas admixtures in the near-water layer of the atmosphere of Lake Baikal (Ship-based expedition, September 2021). *Atmos. Ocean. Opt.* **2022**, *35*, 48–57. [[CrossRef](#)]
17. Izmesht'eva, L.R.; Moore, M.V.; Hampton, S.E.; Ferwerda, C.J.; Gray, D.K.; Woo, K.H.; Pislegina, H.V.; Krashchuk, L.S.; Shimaraeva, S.V.; Silow, E.A. Lake-wide physical and biological trends associated with warming in Lake Baikal. *J. Great Lakes Res.* **2016**, *42*, 6–17. [[CrossRef](#)]
18. Panchenko, M.V.; Belan, B.D.; Shamanaev, V.S. Investigation of Lake Baikal environment with airplane-laboratory of the Institute of Atmospheric Optics SB RAS. *Atmos. Ocean. Opt.* **1997**, *10*, 463–472. (In Russian)
19. Dieudonné, E.; Chazette, P.; Marnas, F.; Totems, J.; Shang, X. Lidar profiling of aerosol optical properties from Paris to Lake Baikal (Siberia). *Atmos. Chem. Phys.* **2015**, *15*, 5007–5026. [[CrossRef](#)]
20. Balin, Y.S.; Bairashin, G.S.; Kokhanenko, G.P.; Penner, I.E.; Samoilova, S.V. LOSA-M2 aerosol Raman lidar. *Quantum Electron.* **2011**, *41*, 945–949. [[CrossRef](#)]
21. Nasonov, S.; Balin, Y.; Klemasheva, M.; Kokhanenko, G.; Novoselov, M.; Penner, I.; Samoilova, S.; Khodzher, T. Mobile aerosol Raman polarizing lidar LOSA-A2 for atmospheric sounding. *Atmosphere* **2020**, *11*, 32. [[CrossRef](#)]

22. Available online: <https://www.hamamatsu.com/eu/en/product/optical-sensors/pmt/pmt-module/current-output-type/H11526-20.html> (accessed on 25 May 2023).
23. Slesar, A.S.; Chaikovskiy, A.P.; Ivanov, A.P.; Denisov, S.V.; Korol, M.M.; Osipenko, F.P.; Balin, Y.S.; Kokhanenko, G.P.; Penner, I.E. Fotodetector modules for CIS-LiNet lidar network stations. *Atmos. Ocean. Opt.* **2013**, *26*, 1073–1081.
24. Available online: <https://www.hamamatsu.com/eu/en/product/optical-sensors/pmt/pmt-module/current-output-type/H11706P-40.html> (accessed on 25 May 2023).
25. Samoilova, S.V.; Balin, Y.S.; Kokhanenko, G.P.; Penner, I.E. Investigations of the vertical distribution of troposphere aerosol layers based on the data of multifrequency raman lidar sensing. Part I. Method of optical parameter retrieval. *Atmos. Ocean. Opt.* **2009**, *22*, 302–315. [[CrossRef](#)]
26. Samoilova, S.V. Simultaneous reconstruction of the complex refractive index and the particle size distribution function from lidar measurements: Testing the developed algorithms. *Atmos. Ocean. Opt.* **2019**, *32*, 628–642. [[CrossRef](#)]
27. Ångström, A. Circumsolar radiation as a measure of the turbidity of the atmosphere. Part 2. *Appl. Opt.* **1974**, *13*, 1477–1480. [[CrossRef](#)] [[PubMed](#)]
28. Available online: <http://meteosap.ru/catalog/amk-03/> (accessed on 25 May 2023).
29. Draxler, R.R.; Rolph, G.D. HYbridSingle-Particle Lagrangian Integrated Trajectory Model (Dataset). Available online: <http://www.arl.noaa.gov/ready/hysplit4.html> (accessed on 17 May 2023).
30. Stull, R.B. *An Introduction to Boundary Layer Meteorology*; Kluwer Academic: Dordrecht, The Netherlands, 1988; pp. 1–28.
31. Burman, E.A. *Mestnye Vetry [Local Winds]*; Gidrometeoizdat: Leningrad, Russia, 1969; pp. 3–73. (In Russian)
32. Nasonov, S.; Balin, Y.; Klemasheva, M.; Kokhanenko, G.; Novoselov, M.; Penner, I. Peculiarities of the vertical structure of atmospheric aerosol fields in the basin of Lake Baikal according to lidar observations. *Atmosphere* **2023**, *14*, 837. [[CrossRef](#)]
33. University of Wyoming. Available online: <http://weather.uwyo.edu/upperair/sounding.html> (accessed on 20 July 2023).
34. Available online: <http://fires-dv.kosmosnimki.ru/> (accessed on 17 May 2023).
35. Dementeva, A.; Zhamsueva, G.; Zayakhanov, A.; Tsydygov, V. Interannual and seasonal variation of optical and microphysical properties of aerosol in the Baikal region. *Atmosphere* **2022**, *13*, 211. [[CrossRef](#)]
36. Arctic and Antarctic Research Institute. Available online: [http://old.aari.ru/odata/\\_d0010.php](http://old.aari.ru/odata/_d0010.php) (accessed on 25 May 2023).

**Disclaimer/Publisher’s Note:** The statements, opinions and data contained in all publications are solely those of the individual author(s) and contributor(s) and not of MDPI and/or the editor(s). MDPI and/or the editor(s) disclaim responsibility for any injury to people or property resulting from any ideas, methods, instructions or products referred to in the content.